EPJ Web of Conferences **364**, 01005 (2026) https://doi.org/10.1051/epjconf/202636401005
Quark Matter 2025

Recent results from the PHENIX experiment

Roli Esha[1,*] for the PHENIX Collaboration
[1]Department of Physics and Astronomy, Stony Brook University, Stony Brook, NY, USA

Abstract. The PHENIX experiment at the Relativistic Heavy Ion Collider, retired in 2016, has continued to deliver impactful results. This proceeding highlights recent developments across several key areas that provide essential benchmarks for theoretical models and contribute substantially to our understanding of Quantum Chromodynamics (QCD).

1 Introduction

The PHENIX experiment at the Relativistic Heavy Ion Collider has been one of the four original detector systems designed to study the properties of strongly interacting matter at high energy density. Although data taking concluded in 2016, the collaboration has continued to produce high-impact results based on the extensive dataset collected over more than a decade of operation. Recent analyses have addressed central topics in heavy-ion physics, including the role of direct photons as probes of the medium, precision measurements of heavy flavor hadrons, systematic studies of light hadrons across collision systems, and new insights from $p + p$ collisions. These results contribute to a deeper understanding of QCD matter and provide essential benchmarks for future experimental and theoretical developments.

2 Small-System Collisions

PHENIX developed a novel method to determine the number of binary nucleon–nucleon collisions using direct photons as a standard candle [1]. Since direct photons are color neutral and do not undergo strong interactions, the scaling factor has been derived empirically from the ratio of direct photon yields in $A + A$ to those in $p + p$ collisions.

This approach has minimized the dependence on the Glauber model. While Glauber estimates agree for central collisions, they systematically underpredict the number of binary collisions in peripheral events as shown in Figure 1(a). By redefining the nuclear modification factor with this method, PHENIX has observed a suppression of about 20% in the 0–5% most central d+Au collisions at $\sqrt{s_{NN}} = 200$ GeV shown in Figure 1(b). Ongoing analyses in p+Au and ^{3}He+Au systems will clarify whether this suppression indicates final state effects in small-system collisions or residual centrality bias.

*e-mail: roli.esha@stonybrook.edu

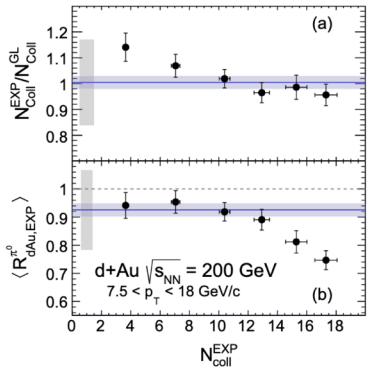

Figure 1. Ratio $N_{\rm coll}^{\rm EXP}/N_{\rm coll}^{\rm GL}$ (a) and the average $R^{\pi^0}_{d{\rm Au,EXP}}$ (b) as a function of $N_{\rm coll}^{\rm EXP}$. Here, $N_{\rm coll}^{\rm EXP} = Y^{\gamma^{\rm dir}}_{d{\rm Au}}/Y^{\gamma^{\rm dir}}_{pp}$, $N_{\rm coll}^{\rm GL}$ is the number of binary nucleon-nucleon from the Glauber model and $R^{\pi^0}_{d{\rm Au,EXP}} = \frac{Y^{\pi^0}_{d{\rm Au}}}{N_{\rm coll}^{\rm EXP} Y^{\pi^0}_{pp}}$ Horizontal and vertical bars are the statistical uncertainties. The values for 0%–100% d+Au collisions at 200 GeV are represented by a solid [blue] line, with the statistical uncertainty given as a band. The scale uncertainties that are common to all data points are shown for the 0%–100% value.

3 The Direct Photon Puzzle

High-statistics Au+Au data at $\sqrt{s_{NN}}$ = 200 GeV has enabled precision studies of direct photons. The elliptic flow, v_2, of direct photons is measured in 10% centrality bins as a function of transverse momentum, p_T [2]. At intermediate p_T (2–3 GeV/c), amplitudes are observed to be as large as those of hadrons, while at $p_T > 10$ GeV/c, where prompt processes dominate, v_2 is consistent with zero.

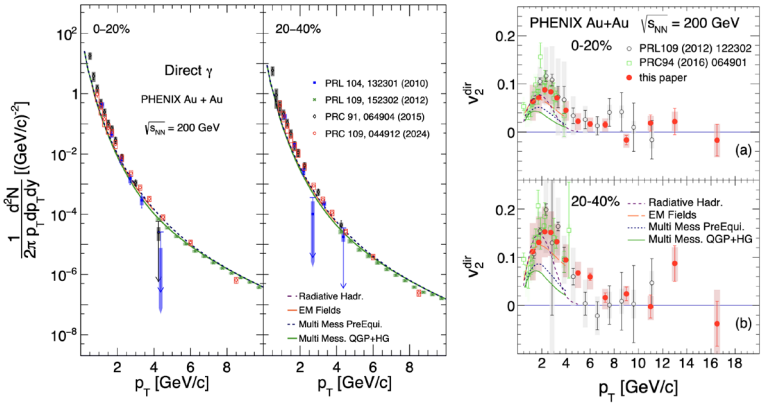

Figure 2. Comparison of the direct photon spectra (left) and azimuthal anisotropy (right) with various theoretical models for 0%–20% and 20%–40% central Au+Au collisions at $\sqrt{s_{NN}}$ = 200 GeV.

Measurement of invariant yields of direct photons as a function of p_T have confirmed earlier measurements with independent methods. Theoretical calculations pre-equilibrium sources and thermal radiations [3], photons from hadronization [4] and magnetic-field effects [5] have systematically underestimated the simultaneous large yield [6] and large flow as observed in data at low p_T, also shown in Figure 2. A consistent theoretical description of these observations remains elusive.

4 Results with the Silicon Vertex Tracker

The VTX has enabled the first measurement of the fraction of B-meson fragmenting to J/ψ in p + $p$collisions at $\sqrt{s}$ = 200 GeV at midrapidity using template fits to displaced-vertex

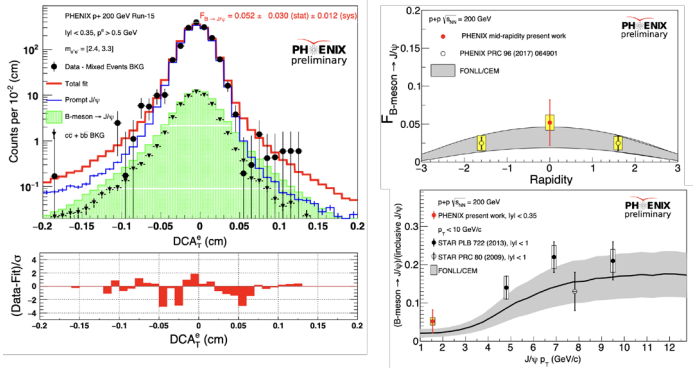

Figure 3. Template fit decomposition used to extract the fraction of B-mesons fragmenting to J/ψ in $p + p$collisions at $\sqrt{s}$ = 200 GeV (left). The comparison of the measured fractions to FONLL+CEM theoretical predictions and to STAR measurements across rapidity (right).

distributions, the decomposition of which is shown in Figure 3 (left). The obtained fractions consistent with FONLL+CEM predictions over a wide rapidity range as shown in Figure 3 (top right) and with STAR measurements (bottom right).

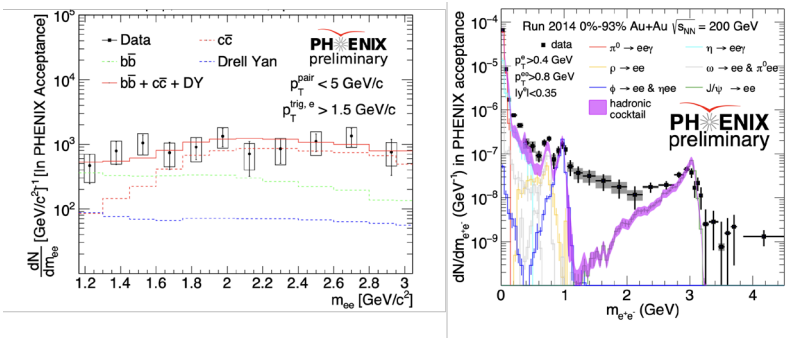

Figure 4. Comparison of dielectron invariant mass spectra after subtraction of hadronic background sources, showing agreement with theoretical predictions from leading-order PYTHIA heavy-flavor and Drell–Yan processes in $p + p$collisions at 200 GeV (left). Early results for Au+Au collisions in the intermediate-mass region compared with the known hadronic cocktail (right).

While the VTX would be a boon for the measurement of dielectron pairs, ~14% radiation length from the same detector poses an enormous challenge for the measurement. Building onto the measurement of pair DCA, PHENIX developed a very effective technique for conversion rejection. Figure 4 (left) shows a good agreement between the dilepton mass spectrum after subtraction of hadronic sources between $\phi < m_{ee} < J/\psi$ with LO PYTHIA heavy-flavor and Drell–Yan contributions in $p + p$ collisions at 200 GeV. Early results of dilepton pair mass distributions in Au+Au collisions to disentangle thermal from heavy-flavor sources in the intermediate-mass region using machine-learning-based background subtraction is shown in Figure 4 (right).

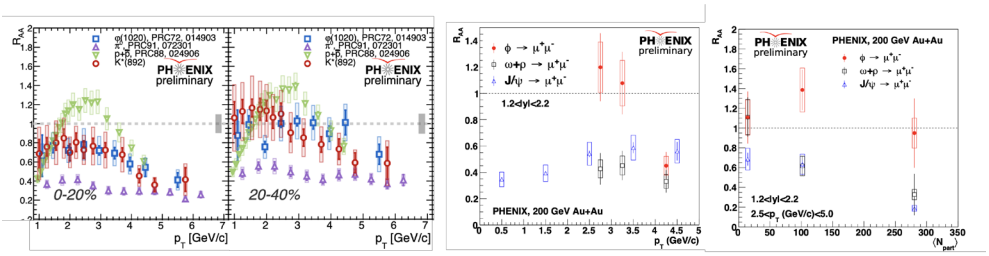

Figure 5. Systematic measurements of π, K, ϕ, ω, K^*, and J/ψ meson production across multiple collision systems highlighting strangeness enhancement and nuclear modification factors for different hadron species at mid- (left) and forward rapidity (right).

5 Light Hadron Measurements

Systematic measurements of π, K, ϕ, ω, and K^* mesons across p+Al, p+Au, d+Au, ^{3}He+Au, Au+Au, and U+U systems is shown in Figure 5 [7, 8]. Strangeness enhancement is revisited via K* at midrapidity and ϕ, and $\omega + \rho$ at forward rapidity. Nuclear modification factors, R_{AA}, shows suppression for $\omega + \rho$, and J/ψ, while ϕ mesons exhibited enhanced yields at forward rapidity. Comparisons across hadron species account for differences driven by recombination, strangeness enhancement, jet-quenching and flow effects for mesons and baryons.

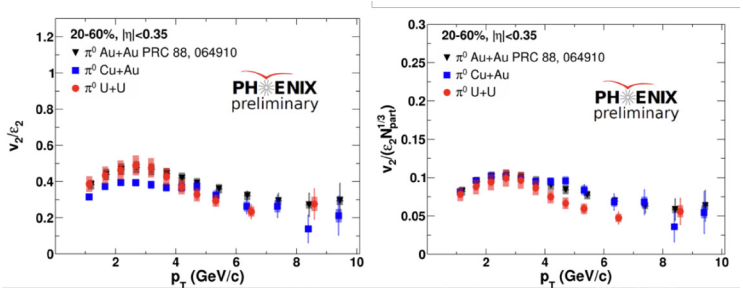

Figure 6. Scaling of elliptic flow coefficient v_2 of neutral pions in Au+Au, Cu+Au, and U+U collisions at 200 GeV.

Elliptic flow, v_2, of neutral pion in Au+Au, Cu+Au, and U+U collisions is shown in Figure 6. v_2 scales with initial ellipticity at high p_T and with $(\epsilon N_{part})^{1/3}$ at low p_T.

6 Results from $p + p$ Collisions

A notable result is the measurement of the cross-section of the η meson upto $p_T \sim 40$ GeV/c in $p + p$ collisions at 510 GeV at midrapidity as shown in Figure 7 with comparisons with the pQCD calculations [9]. These results are important inputs in the global fits to obtain the fragmentation function.

At $\sqrt{s} = 200$ GeV, the normalized yield of J/ψ as a function of normalized charge density at forward rapidity is shown in Figure 8 [10]. The data can only be described by invoking multi parton interactions in Pythia8.

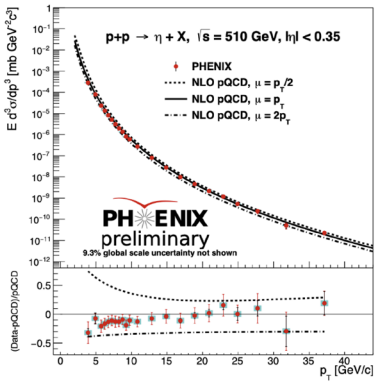

Figure 7. Measured cross-sections of η-meson production in $p + p$ collisions at 510 GeV at midrapidity, compared with pQCD calculations.

The measurement of inclusive jet spectra and substructure observables are shown in Figure 9 [11]. The observation that the theoretical predictions overestimate the data can be attributed to the procedure that translates the partonic cross-section to hadronic cross-sections and relies heavily on modeling.

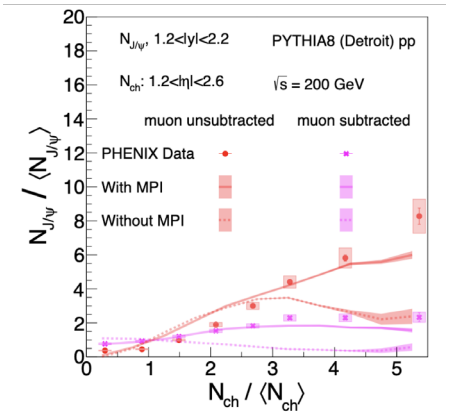

Figure 8. Normalized yield of J/ψ as a function of normalized charge density at forward rapidity in $p + p$ collisions at 200 GeV.

7 Summary

PHENIX has remained scientifically productive well beyond the end of data collection. Novel direct-photon methods have removed Glauber-model dependence in small-system analyses. Multidimensional inputs to the direct-photon puzzle, precision heavy-flavor and dielectron measurements with the VTX, systematic light-hadron studies, and key results from $p + p$collisions have enriched the global QCD dataset. More than a decade after data taking, PHENIX has continued to deliver impactful results and state-of-the-art analyses.

References

[1] N.J. Abdulameer et al. (PHENIX), Disentangling Centrality Bias and Final-State Effects in the Production of High-pT Neutral Pions Using Direct Photon in d+Au Collisions at sNN=200 GeV, Phys. Rev. Lett. **134**, 022302 (2025), 2303.12899. 10.1103/PhysRevLett.134.022302

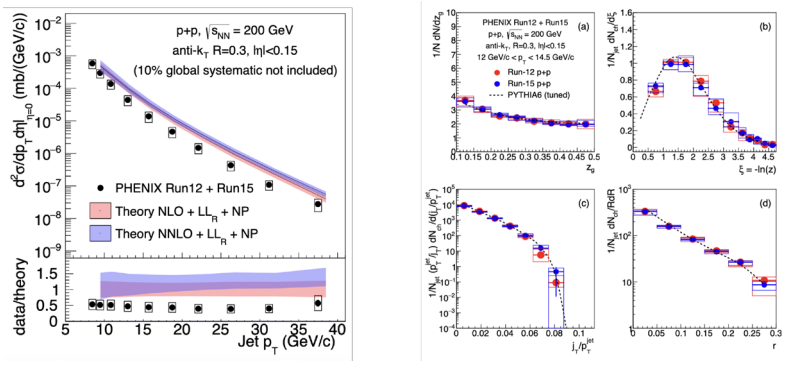

Figure 9. Inclusive jet spectra and substructure observables in $p + p$ collisions at 200 GeV.

[2] N.J. Abdulameer et al. (PHENIX), Azimuthal anisotropy of direct photons in Au+Au collisions at $\sqrt{s_{NN}}$ = 200 GeV (2025), 2504.02955

[3] C. Gale, J.F. Paquet, B. Schenke, C. Shen, Multimessenger heavy-ion collision physics, Phys. Rev. C **105**, 014909 (2022), 2106.11216. 10.1103/PhysRevC.105.014909

[4] H. Fujii, K. Itakura, K. Miyachi, C. Nonaka, Photon Production in High-energy Heavy-ion Collisions: Thermal Photons and Radiative Recombination, Acta Phys. Polon. Supp. **16**, 1 (2023). 10.5506/APhysPolBSupp.16.1-A130

[5] J.A. Sun, L. Yan, Estimating the magnetic field strength in heavy-ion collisions via direct photon elliptic flow, Phys. Rev. C **109**, 034917 (2024), 2311.03929. 10.1103/PhysRevC.109.034917

[6] N.J. Abdulameer et al. (PHENIX), Nonprompt direct-photon production in Au+Au collisions at sNN=200 GeV, Phys. Rev. C **109**, 044912 (2024), 2203.17187. 10.1103/PhysRevC.109.044912

[7] N.J. Abdulameer et al. (PHENIX), Identified charged-hadron production in p+Al, He3+Au, and Cu+Au collisions at sNN=200GeV and in U+U collisions at sNN=193GeV, Phys. Rev. C **109**, 054910 (2024), 2312.09827. 10.1103/PhysRevC.109.054910

[8] N.J. Abdulameer et al. (PHENIX), Low-mass vector-meson production at forward rapidity in $p + p$ and Au+Au collisions at $\sqrt{s_{NN}}$ = 200GeV (2025), 2507.04463

[9] N.J. Abdulameer et al. (PHENIX), Cross sections of η mesons in $p + p$ collisions at forward rapidity at $\sqrt{s}$ = 500 GeV and central rapidity at $\sqrt{s}$ = 510 GeV (2025), 2507.04896

[10] N.J. Abdulameer et al. (PHENIX), Multiplicity dependent J/ψ and $\psi(2S)$ production at forward and backward rapidity in p+p collisions at $\sqrt{s}$ = 200 GeV (2024), 2409.03728

[11] N.J. Abdulameer et al. (PHENIX), Measurement of inclusive jet cross section and substructure in p+p collisions at s=200 GeV, Phys. Rev. D **111**, 112008 (2025), 2408.11144. 10.1103/hpm9-qfp6